

EXPERIMENTAL STUDY ON EFFECT OF ENERGY DISTRIBUTION ON TRANSVERSE PHASE SPACE TOMOGRAPHY

H. Zen[#], H. Ohgaki, K. Masuda, T. Kii, T. Shiiyama, S. Sasaki, N. Okawachi, M. Nakano, K. Yoshikawa, T. Yamazaki

Institute of Advanced Energy, Kyoto University, Gokasho, Uji, Kyoto, 611-0011, Japan.

Abstract

Effect of energy distribution of electron beam on transverse phase space distribution obtained by the use of tomographic method is described. Experimental phase space distribution of electron beam with low energy-tail has weak and scattered halo, which does not appear in the case of the beam without the tail. The result is consistent with the result of previous simulations. An iterative elliptical analysis is proposed to extract the beam parameters of main component from distorted phase space image. It was shown in simulation that the method could extract the beam parameters of main component from distorted image. And then, the method was applied to experimental results. As the results, the vertical and horizontal emittances at the upstream and downstream of energy filter are agreed well.

INTRODUCTION

It is indispensable to measure not only emittances but also phase space distributions of electron beams to evaluate and optimize the performance of electron guns. Transverse phase space tomography [1] is powerful method especially for non-Gaussian beam, because the method directly reconstructs the phase space distribution of electron beams. However, the assumption of mono-energy is essential for the method. Thermionic rf guns inherently produce electron beams which have large energy spread (about 10 to 15 percent) and low energy tail, and the energy distribution distorts measured phase space distribution obtained by tomographic method.

We have evaluated the effect of energy distribution on the tomographic method by numerical simulations [2]. It was found that the signals of low energetic electrons are reconstructed as weak and scattered signals on wide region of reconstructed phase spaces, and those signals lead to large errors in beam parameters. On the other hand, it was also found that the energy spread of main component have no large effect on the method even if the energy spread is 15 percent.

The effect was evaluated by comparison of the reconstructed image from the upstream and that from the downstream of an energy filtering section. Furthermore for the beam just after the gun, we introduced an elliptical analysis to remove the effect of low energy tail in order to obtain correct beam parameters at the gun exit by the tomographic method.

EXPERIMENTAL SETUP

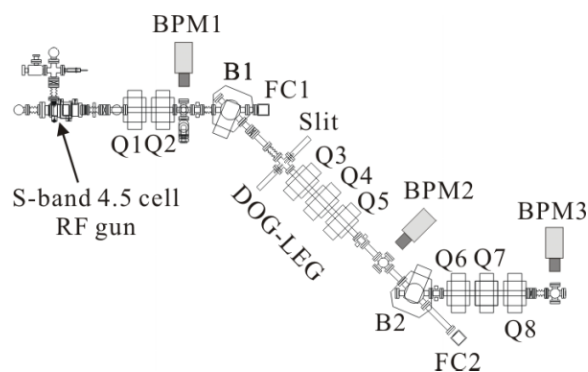


Figure 1: Experimental arrangement.

Figure 1 shows the experimental setup. A dispenser cathode of disk shape with 6 mm diameter is mounted in the first half cell of our 4.5 cell RF gun. To reduce backstreaming electrons [3], transverse magnetic field was applied with a dipole magnet located just before the rf gun [4]. The beam profile monitor (BPM) consist of a fluorescence screen (Cr doped Al_2O_3) and a CCD camera, and its spatial resolution is 0.05 mm.

Dog-leg section in Fig. 1, which consisted of two dipole magnets, a slit, and a quadrupole triplet, worked as an energy filter and its energy resolution is about 5 percent.

The quadrupole magnet 1 (Q1) and the BPM1 are used to measure the phase space distributions at the upstream of the energy filter, and the Q6 and BPM3 are used to measure them at the downstream.

Beam parameters in the experiments are shown in Table 1, and the energy distribution obtained with bending magnet 1 (B1) and Faraday cup 2 (FC2) is shown in Fig. 2. Unfortunately signals of FC2 of low energy tail (less than 7 MeV) were too weak to be separated from the electric noise. However, the existence of low energy tail has been predicted in the previous simulation for our rf gun [2].

For tomographic reconstruction, we used ordered-subset expectation maximization algorithm [5] whose advantage is that there is no artefact on reconstructed images.

[#]heishun@iae.kyoto-u.ac.jp

Table 1: Beam parameters in experiments

	@ BPM1	@ BPM3
Macro pulse duration	1.6 μ sec	1 μ sec
Total charge	300 nC	100 nC
Charge per bunch	66 pC	35 pC
Peak Energy	9.2 MeV	

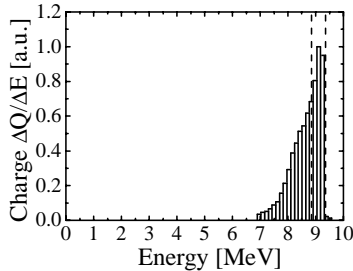


Figure 2: Measured energy spectrum of the electron beam at the exit of gun (dashed lines indicate the energy acceptance of dog-leg section).

RESULTS OF EXPERIMENT

The results of experiments are shown in Fig. 3 and 4. Before reconstruct the Q1 result, background signals were subtracted. At the Q1 entrance horizontal and vertical normalized emittances are evaluated as 82 and 44 π mm mrad, respectively, while those are 12 and 6.9 π mm mrad at the Q6 entrance.

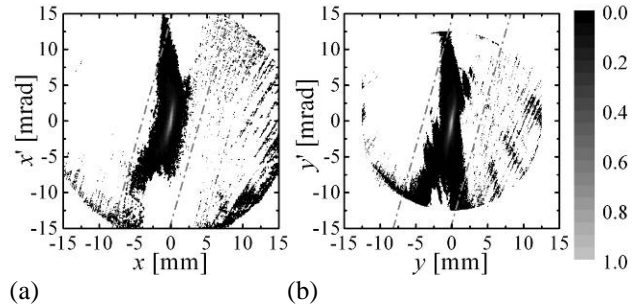
There are weak and scattered signals in Fig. 3 where the electron beam had a low energy tail, while such signals are not seen in Fig. 4. It is consistent with previous numerical studies that the phase space distributions for the beam with low energy tail are severely distorted.

In Fig. 3, the region between dashed lines indicates where electrons can exist and the region is calculated from aperture of the gun exit (4 mm in diameter) and the distance between the gun exit and Q1 (27.5 cm). The signals in outside of the region are miss-reconstructed signals due to difference from assumed energy at least.

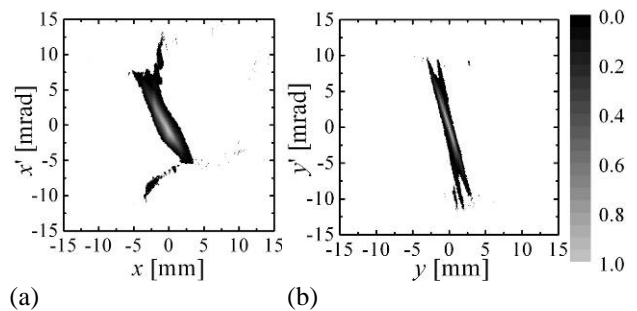
Therefore, it was shown in experiment that the signals from low energy tail are reconstructed as weak and scattered signals. We can not obtain correct phase space distributions by using tomographic method if low energy tail is contained in an electron beam.

REMOVAL OF LOW ENERGY SIGNALS

Amount of low energy electrons produced by a thermionic rf gun is much fewer than amount of electrons included in main component, and low energy electrons are reconstructed wider and weaker than true distribution. So intensity of low energy electrons on reconstructed phase space is much weaker than intensity of electrons included in main component. However, the emittance calculation is strongly affected by the tail. Therefore, we need to remove the weak signals which are originated from low energy electrons to obtain correct beam parameters by the tomographic method.



(a) (b)
Figure 3: Phase space distributions at the entrance of Q1 (dashed lines indicate the regions where electrons can exist and are calculated from experimental geometry). (a) Horizontal and, (b) vertical.



(a) (b)
Figure 4: Phase space distributions at the entrance of Q6 measured by tomographic method, (a) Horizontal and (b) vertical.

Procedure of Iterative Elliptical Analysis

To remove the weak signals produced by low energy electrons automatically, we introduced an iterative elliptical analysis (IEA) [6]. The procedure is:

- I : Calculate $\langle x^2 \rangle$, $\langle x'^2 \rangle$ and $\langle xx' \rangle$ from reconstructed phase space distribution.
- II : Draw ellipse defined by Eq. 1 on reconstructed phase space.

$$\langle x^2 \rangle x'^2 + 2\langle xx' \rangle xx' + \langle x'^2 \rangle x^2 = 9\epsilon^2 \quad (1)$$

Eq. (1) represents the 99 percent ellipse of Gaussian distributions.

- III: Calculate $\langle x^2 \rangle$, $\langle x'^2 \rangle$ and $\langle xx' \rangle$ from reconstructed phase space distribution only in the ellipse.
- IV : In the same way with step II and III, draw ellipse using newly calculated $\langle x^2 \rangle$, $\langle x'^2 \rangle$ and $\langle xx' \rangle$ in step
- V : Repeat step III and IV until $\langle x^2 \rangle$, $\langle x'^2 \rangle$ and $\langle xx' \rangle$ sufficiently converge.

Simulation of Iterative Elliptical Analysis

Reliability of IEA was examined by using numerical simulation. We gave the Gaussian-shaped phase space distribution with the energy distribution shown in Fig. 5 as original distribution and simulated the experiment of tomographic method. In this simulation, space charge effect was neglected, since it was not significant for our thermionic rf gun. As the result of the simulation, a distorted phase space distribution was reconstructed (Fig. 6). Although weak and scattered signals exist in the figure,

strong signals in the center are looked similar to the original phase space distribution (Fig.5).

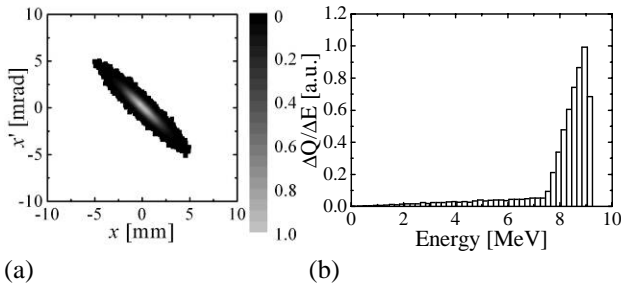


Figure 5: Original distribution of numerical simulation, (a) phase space distribution (normalized emittance = 3.3π mm mrad, $\alpha = 2.9$ and $\beta = 3.1$ m), (b) energy spectrum.

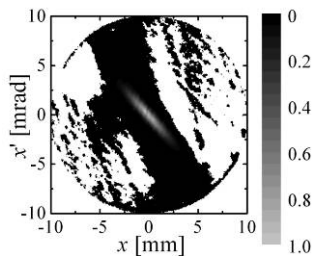
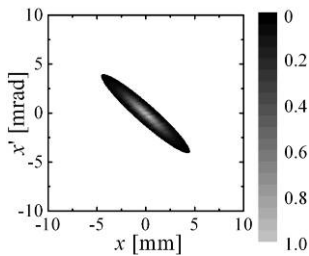
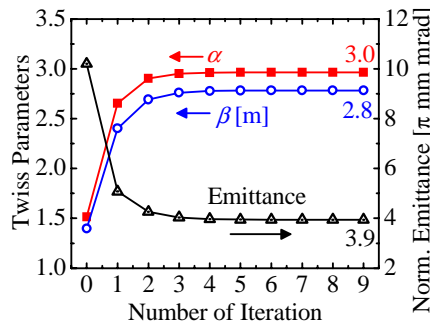


Figure 6: A result of numerical simulation (normalized emittance = 10π mm mrad, $\alpha = 1.5$ and $\beta = 1.4$ m).



(a)



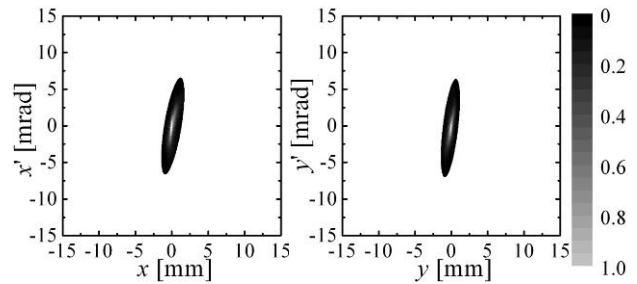
(b)

Figure 7: Result of IEA applied to simulation result, (a) phase space distribution (normalized emittance = 3.9π mm mrad, $\alpha = 3.0$ and $\beta = 2.8$ m), (b) convergence of emittance and Twiss parameters.

The result of IEA applied to the Fig.6 is shown in Fig. 7. The normalized emittance and Twiss parameters gradually converged to 3.9π mm mrad, $\alpha = 3.0$ and $\beta = 2.8$ m, respectively as iteration number increased. The beam parameters of original distribution were normalized emittance = 3.3π mm mrad, $\alpha = 2.9$ and $\beta = 2.8$ m. Since each error in beam parameters is less than 20 percent, this method is reliable.

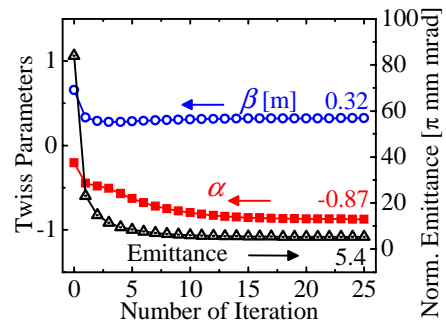
Application of IEA to Experimental Result

IEA was applied to experimental results at the entrance of Q1 and the results are shown in Fig. 8. A center core of reconstructed phase space distribution was successfully obtained and beam parameters sufficiently converged. As results of application of IEA, measured horizontal and vertical emittances were 5.4 and 4.7π mm mrad, respectively.

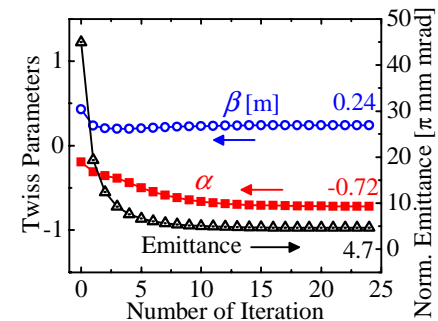


(a)

(b)



(c)



(d)

Figure 8: Results of IEA applied to experimental results. (a) Horizontal phase space distribution of horizontal direction. (b) Vertical phase space distribution. (c) and (d) convergence of horizontal and vertical beam parameters, respectively.

The IEA was also applied to experimental results at the Q6 entrance and measured emittances of horizontal and vertical directions at the Q6 entrance were 7.4 and 4.3 π mm mrad, respectively. Measured emittances of vertical direction at the Q1 and Q6 entrance agreed well. However, emittances of horizontal direction did not agree well. The reason of this disagreement was the non-zero horizontal dispersion in the Dog-leg section.

Reliability and an ability of IEA were confirmed both in simulation and experiment. We are now planning to do more experiments under various conditions of the gun in order to evaluate the accuracy of IEA quantitatively. Comparison of transverse phase space distribution with the slit methods will be useful, since the methods are not suffered from energy distribution.

SUMMARY

To study the effect of energy distribution to transverse phase space tomography, experimental results at the upstream and downstream of the energy filter were compared. As the result, the low energy electrons are reconstructed as weak and scattered signals, which are predicted by previous numerical investigation.

To remove the signals from low energy electrons, IEA was introduced and examined. By a numerical simulation,

the validity of the analysis was shown. IEA was applied to experimental results at the upstream of energy filter and compared with the experimental results at the downstream of the filter. The emittances of vertical direction at the upstream and downstream of energy filter agreed well, although horizontal ones were not due to non zero horizontal dispersion in the Dog-leg section. Consequently, reliability and an ability of IEA were shown both in simulation and in experiment.

REFERENCES

- [1] C.B.McKee, et al., NIM A358, 1995, p.264.
- [2] H.Zen, et al., Proc. of FEL2005, 2006, p.592.
- [3] T.Kii, et al., Proc. of FEL2005, 2006, p.584.
- [4] T.Kii, et al., NIM A507, 2003, p.340.
- [5] H.M. Hudson, et al., *IEEE. Trans. Med. Imaging*, **13**, 1994, p.601.
- [6] H.Zen, et al, "Transverse phase space measurement using tomographic method", conference proceedings of SRI2006, in press.